Lab on a Chip

Accepted Manuscript

ROYAL SOCIETY OF CHEMISTRY

www.rsc.org/loc

Journal Name

RSCPublishing

ARTICLE

Point of care diagnostics in ricin exposure

Cite this: DOI: 10.1039/x0xx00000x

Mohamed Lemine Youba DIAKITE[a,b], Jérôme ROLLIN [c], Dorothée JARY[a], Jean BERTHIER [a], Chantal MOURTON-GILLES [d], Didier SAUVAIRE [d], Cathy PHILIPPE [e], Guillaume DELAPIERRE [a], and Xavier GIDROL *[b,f]

Received 00th January 2012,
Accepted 00th January 2012

DOI: 10.1039/x0xx00000x

www.rsc.org/

A long-sought milestone in the defense against bioterrorism is the development of rapid, simple, and near-patient assays for diagnostic and theranostic purposes. Here, we present a powerful test based-on a host response to a biological weapon agent, namely ricin-toxin. A signature for exposure to ricin was extracted and characterized in mice and then integrated into a plastic microfluidic cartridge. This enabled early diagnosis of exposure to ricin in mice using a drop of whole blood in less than 1 h 30 min. The cartridge stores the reagents and implements all of the steps of the analysis, including mRNA extraction from a drop of blood, followed by tens of parallel RT-qPCR reactions. The simple and low-cost microfluidic cartridge developed here may find other applications in point of care diagnostics.

Introduction

Because of its high toxicity and easy production, ricin is a potent poison that poses an increasing bioterrorism threat to the world. Made from the seeds of the castor bean plant (Ricinus communis), this deadly toxin protein works by inactivating ribosomes, the primary sites in cells for protein synthesis [1]. Symptoms can appear as early as 4 hours and as late as 24 hours after exposure, and death can occur between one and a half to three days after exposure. The toxicity of ricin is species-dependent and varies according to the dose and the route of administration (e.g., inhalation, ingestion, or injection)[2]. To date there is no antidote to ricin. In emergency conditions arising from ricin poisoning on a large scale, early diagnosis and triage for therapeutic orientation are necessary to limit mass casualties. Consequently, it is crucial to detect exposure to ricin-toxin in victims as soon as possible and, ideally, before any clinical symptoms are present.

Immunoassays, which generally rely on antibody recognition of the toxin, are the most common approach currently being used for ricin detection. They are used in a variety of formats, including enzyme-linked immunosorbent assays (ELISA) and immunoprecipitation [3] [4], electroluminescence assays [5], fluorescence-based flow cytometry [6], optical waveguide sensors [7], surface plasmon resonance (SPR) [8], photonic microring resonator [9], and immuno-PCR[10]. Although they are suited for detecting ricin in the environment, immunoassays have several limitations for medical diagnosis in the case of bioterrorist attacks as well as for therapeutic purposes. For example, very low concentrations of ricin are difficult to detect in medical samples, and the development of specific, stable and robust antibodies for ricin is still a challenge [11][12][13]. Furthermore, selecting the most relevant body fluid to immunoassay for the toxin is not so obvious. Finally, the adverse effects triggered by ricin may vary from one individual to the next, limiting the usefulness of antibody-based ricin detection for therapeutic orientation.

Here, we report a new approach based on toxicogenomics [14] [15] for diagnosing ricin exposure in the blood of putative victims of an accidental or terrorist attack-related exposure. We hypothesized that the presence of the toxin in a host and its first adverse effects will trigger changes in the gene expression profile in the peripheral blood of the exposed person. Therefore, expression profiling in the blood of suspected victims should facilitate both early diagnosis and therapeutic orientation.

Isogenic mice received ricin through intranasal and intravenous exposure. Genome-wide gene expression profiling in the whole blood of the exposed mice was compared with vehicle treated mice to extract and characterize an exposure signature. To the best of our knowledge, this is the first implementation of toxicogenomics approaches to probe the body's response to ricin exposure.

Emergency medicine requires rapid and portable "near patient" assays [16]. Microfluidic systems provide numerous advantages in this regard, including portability, economies of scale, parallelization

and automation, and increased sensitivity and precision, all of which come from the use of small volume reactions. Considerable effort has been directed toward developing integrated and scalable analysis on chips, particularly in single cell genetics [17] [18]. However, in most cases, this integration involves PDMS chips, which are not suitable for "point of care" (POC) applications because of difficulties with the storage of reagents and devices and with commercialization [19][20]. Plastic chips, such as PMMA (poly[methyl methacrylate]) chips, do not have these limitations. To make the ricin exposure diagnosis assay readily available to patients in an emergency situation related to either a bioterrorism attack or an accidental exposure, the assay developed here has been integrated with a PMMA microfluidic cartridge that is dedicated to expression profiling. This new cartridge stores the reagents and implements all of the process steps for ricin exposure-diagnosis and therapeutic orientation of the victims, ranging from sample preparation (i.e., extraction of mRNA from 10 µl of whole blood) to performing tens of RT-qPCR reactions in parallel in less than 1 h 30 min.

Experimental

In vivo experiments

All the animal studies were conducted at the French National Agency for Security of Medicines and other health products (ANSM) animal care facility**,** with the authorization of the Languedoc Roussillon ethics committee, according to European regulations.

Six-week-old BALB/C mice were purchased from Charles River Laboratories, and three groups were established to extract and characterize the signature of ricin exposure. The first BALB/C mice group received ricin, the second untreated group received a vehicle, and the third group received enterotoxin B toxin. The ricin treated group consisted of a total of eighty-six mice (n=86) that received ricin either intravenously (IV) or through respiration (IN). The LD50 values were determined to be 3.2 µg/kg and 5.88 µg/kg, respectively, for IN and IV injection. Of eighty-six mice, thirty-seven mice (n=37) received ricin by IV injection at various doses (1 µg/kg for n=10; 2 µg/kg for n=8; 4 µg/kg for n=10; and 6 µg/kg for n=9), and forty-nine mice (n=49) received ricin by IN injection at the LD50 dose. Blood samples were collected between 24 and 30 hours after exposure for the IV injected-mice and 4 hours (n=10), 8 hours (n=10), 24 hours (n=10), 48 hours (n=11), and 72 hours (n=7) after exposure for the IN injected-mice. The Enterotoxin B treated group is consisted of fifty-five mice (n=55) that received enterotoxin B by IN injection at the LD50 dose, which was determined to be 1 mg/kg. Blood samples were collected 4 hours, 8 hours, 24 hours, 48 hours, and 72 hours after exposure. Lastly, the untreated group of mice consisted of thirty-two mice (n=32) that were exposed to vehicle only as a control.

After exposure, every mouse was anesthetized, and its blood was collected directly from the heart and was immediately processed with Mouse ribopure blood RNA isolation kit (Life Technologies, France). Total RNA was extracted as per the manufacturer's instructions for further transcriptome studies (see the transcriptome studies section below).

For the validation of the ricin signature in the microfluidic cartridge by RT-qPCR reactions, six week-old Swiss mice (IOPS CD1) were purchased from Janvier Labs (St Berthevin, France). The mice were housed in a controlled and enriched microenvironment under a 12 hours light-dark cycle and fed a standard diet *ad libitum.* All the housing conditions were in accordance with European directive 2010/EU/63 and in respect of the quality norm ISO17025. Ricin was administered by intranasal instillation, and the LD50 value was determined to be 0.536 µg/Kg. Two groups of mice were used. The first group was exposed to intranasal intoxication with ricin at the LD50, and the second group received vehicle only as a control. Blood samples were collected from the abdominal aorta 24 hours, 48 hours, and 96 hours later and were collected in PAXgene Blood RNA Tubes (Becton, Dickinson Diagnostics, France).

Blood collection

This work is the first implementation of a new approach for ricin exposure diagnosis based on intracellular RNA analysis from whole blood. It was designed to diagnose ricin exposure using a small volume of whole blood from exposed victims for point of care testing in emergency situations. However, a major challenge in this type of testing is the instability of intracellular RNA, which rapidly degrades within hours after blood collection. Furthermore, certain species of RNA, through the process of gene induction, increase in vitro after blood collection. Both in vitro RNA degradation and gene induction can lead to under- or overestimation of in vivo relative gene transcript numbers. For this first proof-of-concept, our aim was to validate the principle of the diagnosis itself and its integration in a simple plastic cartridge compatible with mass production, reagent embedding and storage. Thus, to decouple possible causes of error in the mRNA profiles, blood samples from ricin treated and untreated IOPS CD1 mice were collected in PAXgene Blood RNA tubes, which contain an additive that stabilizes the in vivo gene transcription profile by reducing in vitro RNA degradation and minimizing gene induction. However, the PAXgene tubes require 2.5 mL blood, higher than the volume of blood that can be collected from mice (between 100 µl and 900 µl). Consequently, we calculated the blood to Paxgene additive ratio and maintained it exactly to preserve RNA integrity, as reported in a previous study[21]. After collection, the blood samples were stored at -80°C until use.

Transcriptome studies

The microarray analysis was performed with the RNG-MRC mouse array, which contains 24109 gene-specific oligonucleotide probes, as described in Le Brigand *et al.* [22]. Pangenomic microarrays were printed using the human RNG-MRC oligonucleotide collection with the Microgrid II (BIOROBOTICS, Cambridge, UK) on commercial Nexterion Slide H (Schott, Mainz, Germany) coated with hydrogel, and they were processed according to the manufacturer's instructions. Data concerning the probe sets can be directly downloaded from the MEDIANTE home page http://www.microarray.fr. For the transcriptome study, we used RNA samples obtained from whole blood samples from BALB/C mice that were exposed or not exposed to ricin. The integrity of all RNA samples was assessed with the RNA 6000 Nano LabChip kit

(Agilent, Palo Alto, CA). Labelled aRNA were amplified from 1 µg of total RNA from each sample with the Amino Allyl MessageAmp TM II aRNA kit (#1753) (Ambion, Austin, TX). Cy3 and Cy5 labelled aRNA was purified, fragmented with 10 µL of 25X fragmentation buffer (Agilent) in 240 µl of RNase free water, and mixed with the Cy5 and Cy3 from non-treated cells. 250 µl of 2X hybridization buffer (Agilent) was added at room temperature, and the mixture was incubated for one hour at 50°C. The slides were prehybridized for one hour at room temperature and then hybridized for 17 hours at 60°C. The slides were washed in 6X SSC + 0.005% triton X-100 for 10 minutes in the dark, 0.1 X SSC + 0.005% triton X-100 for 5 minutes in the dark and then dried using an air spray.

Statistical analysis

The statistical analysis was based on two dye swaps (*i.e.*, four arrays, each containing 24109 probes and 544 controls) for each ricin concentration. The controls were used to assess the quality of hybridization but were not included in the statistical test or in the graphical representation of the results. The raw data were GenePix Results (GPR). No background was subtracted. After manually checking the intensity values for each slide, we excluded from the analysis any genes that were flagged during the GenePix analysis, as well as outlier genes (*i.e.*, genes that had a ratio higher than 1.2 or lower than 0.8 on slides corresponding to the hybridization of RNA from mice not exposed to ricin). Our data were then normalized according to the print-tip loess method using the marray R package from Bioconductor. Differentially expressed genes between two adjacent doses of exposure to ricin were determined with the limma R package from Bioconductor. The p-values were adjusted with the Benjamini and Hochberg method [23], which controls the False Discovery Rate (FDR). The lists of genes that were differentially expressed were then identified by applying a cut-off value of 0.01 to the adjusted p-value. We used the 'fold change' (FC) value as the expression value. To define FC, the ratio R of the intensity of a gene from the first tested condition to the intensity of the same gene from second condition tested was calculated. If R is greater or equal to one, then FC equals R. If R belongs to [0, 1[, FC is set to $(- R)^{-1}$. Finally, we used Ingenuity Pathway Analysis (IPA), which relies on the Ingenuity Pathway Knowledge Base (IPKB) (Ingenuity System®, www.ingenuity.com), to further analyze our sets of genes.

Experimental set-up

The developed compact instrument performed pneumatic actuation, thermal control, and fluorescence measurements. It included: 1) a holder for the microfluidic cartridge (HMC), 2) a pressurizing system for the cartridge, 3) a magnet and a mechanical mixer, and finally 4) a camera and LEDs for fluorescence measurements. The HMC consisted of a heating system based-on a Peltier module combined with a PT100 temperature sensor and 5 holes in which the 5 integrated valves in the cartridge were placed for pneumatic actuation. Plastic tubing was used to connect the 5 holes to solenoid actuators, which were controlled by a digital input output card USB (National Instruments). The whole cartridge was pressed against the HMC by a mechanical pressurizing system. Suspensions were injected into the cartridge using a pressure controller (MFCS and FLUIWELL, Fluigent, France). The fluorescence measurements was dedicated to the detection of FAM probe (Excitation 485±20, Emission 525±25). A camera was used to detect the emitted fluorescence.

The florescence measurements, valve actuations and thermal cycling were operated using homemade software. A gentle stirrer system consisting of a rotating arm that gently hit against the adhesive film acted as mechanical mixer.

Suspensions for mRNA isolation and RT-qPCR reactions

The protocol for mRNA isolation from blood was similar to the standard protocol for the mRNA DIRECT™ Kit (Life Technologies, France). It used suspensions for lysis/binding and washing (buffer A and B). The lysis /binding suspension consisted of 150 µl of lysis/binding buffer, 30 µl of mouse blood collected in a Paxgene Tube (equivalent of 10 µl of whole mouse blood), and 6 µl of Dynabeads® oligo-DT, corresponding to a binding capacity of up to 60 ng of poly A+ RNA, which is much larger than the expected expression level of mRNA in 10 µl of blood. The suspension for the RT-qPCR reactions was based-on the SuperScript® III Platinum® One-Step qRT-PCR kit (Life Technologies, France) with the following optimized reagent concentrations: 1X Reaction Mix, 3rxn of Superscript III RT/platinum Taq Mix, 300 units of RNaseOUT™ Recombinant Ribonuclease Inhibitor (Life technologies, France) and 2 mM magnesium (Life technologies, France).

Thermal cycling

The RT-qPCR reactions were thermocycled with the following conditions: 15 min at 50 °C, 2 min at 95 °C, followed by 40 cycles of 15 s at 95 °C and 30 s at 60 °C.

Fluorescence measurements

Fluorescence in the RT-qPCR reaction microchambers was measured by the camera and LEDs through the glass of the clamping system. After each PCR temperature cycle, a fluorescence image of the entire RT-qPCR microchamber area was taken. The images were acquired at 60 °C. The fluorescence intensity in each RT-qPCR microchamber was then measured from the images using image J software to generate real-time amplification curves.

Gene expression quantification

The gene expression profile data were generated from the real-time PCR curves using the comparative threshold cycle (CT) method [24]. This relative gene expression method presents the data of the gene of interest relative to a calibrator or internal control gene. Gapdh gene was used as the internal control here, and a heatmap was generated using the ΔΔCT formula, where ΔΔCT= [(CT gene of interest - CT internal control) sample - (CT gene of interest - CT internal control) calibrator]. The calibrator was the average profile of the untreated samples (control), and all other profiles were compared to this group to evaluate the expression of the gene of interest relative to the internal control in the treated sample compared with the untreated control sample.

Results and discussion

Characterization of a set of genes that indicate exposure to ricin

When exposed to the ricin toxin, the body of the host produces a response that integrates the presence of the toxin and the first pathological consequences triggered by the toxin in the body. We hypothesized that by monitoring changes in expression profiles in the whole blood of exposed animals we would be able to probe this response at the very early stages of intoxication. First, we estimated the median lethal dose (LD50) in BALBC mice after intravenous (IV) or intranasal (IN) exposure to ricin. These doses were 5.9 µg and 3.2 µg of ricin per kilogram, respectively. We then performed genome-wide expression profiling in the blood of approximately 170 mice treated with either ricin or Enterotoxin B, by both IV and IN exposure, and compared the results to profiles obtained from the total blood of control mice treated with the vehicle.

Enterotoxin B is a biotoxin that acts through a similar mechanisms to that of ricin and allows to establish the specificity of the ricin exposure detection. To take into account individual variability, we generated more than 140 expression profiles from each mouse at different time points after exposure to the LD50 for each toxin (**Table 1A**) and at different doses (**Table 1B**). Major changes in the expression profiles were observed as early as 4 h after exposure (**Table 1**).

Among the genes differentially expressed in treated mice compared to the control group, we found genes characteristic of inflammation and genes involved in the translation machinery (**Figure S1**), both of which agree with the known mechanism of action of ricin, thus validating the reality of exposure. We then mix the 140 expression profiles and used a boot strap Monte Carlo Cross Validation (MCCV) to extract the minimal set of genes that will discriminate exposure to ricin or enterotoxin B and that could serve as a signature of ricin exposure (**Figure 1A-B**). The MCCV analysis identified of a set of 27 genes (among the 24109 mouse genes present on microarrays) that indicated exposure to ricin consistently, in 50 times out of 50 tests (**Figure 1C**). These 27 genes were further validated in a blind test, with a new test group of mice (n=28; 5 untreated, 13 ricin treated (10 IN and 3 IV), and 10 enterotoxin B treated) in our partner laboratory. Messenger RNA from the treated mice were coded and then sent to our blind laboratory for expression profiling. Using the 27 gene signature, we were able to properly assign each of the 28 mice, without any error, thus confirming the validity of the signature. Finally, the expression of these 27 genes was verified by RT-qPCR with RNA extracted from each individual mouse.

To date, the most comparable test for ricin exposure diagnosis using immunoassays is immuno-PCR. Immuno-PCR was able to detect the ricin exposure in feces of mice that received a dose of 10µg of ricin per mouse through oral inoculation, and was unable to detect the ricin exposure when the intravenous administration mode was used [10]. This suggest that some components in the body could bind with ricin and interfere in its binding activity[3]. As mentioned above ricin exposure diagnosis based on host response did not have these limitations. We thus were able to detect major changes in the expression profiles at a sub-lethal dose as small as 4µg per kilogram (Table 1B). This correspond to about 80ng of ricin per mouse (weights of mice: 19.5–20 g). This dose is 125 fold more sensitive than immuno-PCR testing.

A)

	Mice analyzed T0 (n = 10)	4h vs T0	8h vs T0	24h vs T0	48h vs T0	72h vs T0
Ricin (IN)	Mice analyzed (n)	10	10	11	11	7
	Gene DE (n)	**7**	**13**	**45**	**168**	**340**
	Venn diagramme	1 6 7	1 12 33	3 42 126	40 128 212	
Enterotoxin B (IN)	Mice analyzed (n)	11	11	11	10	12
	Gene DE (n)	**15**	**148**	**67**	**95**	**416**
	Venn diagramme	0 15 133	108 40 27	34 33 62	20 75 341	

B)

	Mice analyzed T0 (n = 20)	1µg vs T0	2µg vs T0	4µg vs T0	6µg vs T0
Ricin (IV)	Mice analyzed (n)	10	8	10	9
	Gene DE (n)	**0**	**0**	**75**	**909**
	Venn diagramme			2 73 836	

Table 1: Number of genes differentially expressed A) between mice exposed to toxin (intranasal) compared to untreated mice, according to the time of exposure, and B) between mice exposed (intravenously) to different concentrations of ricin compared to untreated mice.

A)

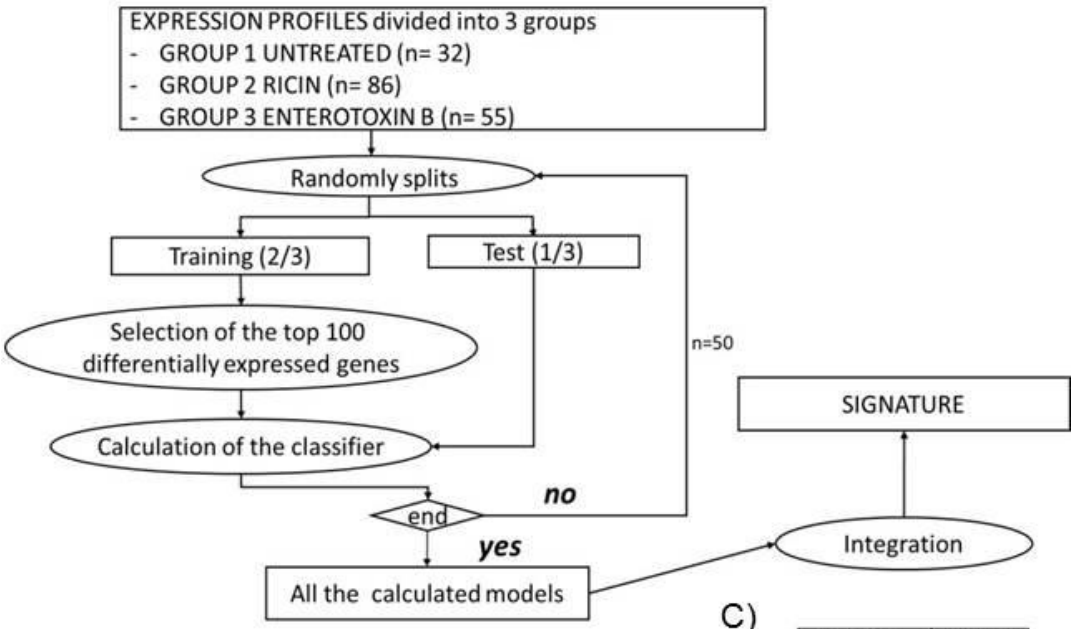

B)

SCORE	NUMBER OF GENES IN SIGNATURE	% ERROR OF THE MODEL	% ERROR BLIND TEST
50	**27**	**0**	**0**
49	33	0	7.142857
48	36	0	7.142857
47	38	0	7.142857
46	42	0	7.142857
45	47	0	10.71429
44	52	0	7.142857
43	53	0	7.142857
42	55	0	7.142857
41	56	0	7.142857
40	58	0	7.142857

C)

SYMBOL	SCORE
1100001G20Rik	50
Alox5ap	50
Anxa2	50
Ccr1	50
Clec4d	50
Crispld2	50
Dusp1	50
Gp49a	50
Hdc	50
Hp	50
Ifitm2	50
Il1b	50
Il1r2	50
Il8rb	50
Mgst1	50
Mmp8	50
Oasl2	50
Prrg2	50
Retnlg	50
S100a6	50
S100a8	50
S100a9	50
Sepx1	50
Slfn1	50
Slpi	50
Stfa2l1	50
Tyrobp	50

Figure1: Characterization of a set of genes that indicate exposure to ricin. A) Monte Carlo Cross-Validation scheme for minimal signature extraction for exposure to ricin. B) Result of the Monte Carlo Cross-Validation analysis. C) List of the 27 genes of the ricin signature in mice. All the primers and probes were purchased from Life Technologies (TaqMan® Gene Expression Assay).

Cartridge design and assembly

The established ricin signature was integrated into a PMMA microfluidic cartridge to bring the test near to patients in a remote environment. To reduce the device complexity, the cartridge was designed to be compatible with commercially available assays using Dynabeads® for the rapid isolation of mRNA and RT-qPCR in one-step, without requiring a mixing step between RT and PCR. The devices were fabricated by micromachining using an Opticmac5 (Aremac polymer, France). Briefly, the 3D microfluidic circuit on the chip consisted of an 80 µl chamber for mRNA extraction from blood and a network of 28 microchambers for the RT-qPCR reactions (**Figure 2**). Each RT-qPCR microchamber had a volume of 1.3 µl. Assembly of the cartridge involved embedding the reagents and then closing the cartridge. To prevent non-specific adsorption, prior to assembly, the micromachined cartridge was soaked in a 1% (w/v) bovine

serum albumin (BSA) solution for 4 hours, rinsed with deionized water, and dried. Next, the primers and probes corresponding to the genes of the established ricin signature (TaqMan® Gene Expression Assays, #4331182, Life Technologies, France) were pipetted into the microchambers. The chambers were then dried at room temperature with sugar for chemical preservation and rapid dissolution by buffer during the assay. Next, the cartridge was closed with a simple adhesive film, thus avoiding complex chemical or thermal bonding processes which are not compatible with the embedded reagents. The fluid control in the cartridge was monitored by pneumatic actuation of the adhesive film, which closes the cartridge. Temperature cycling in the microchambers was performed directly across the adhesive film.

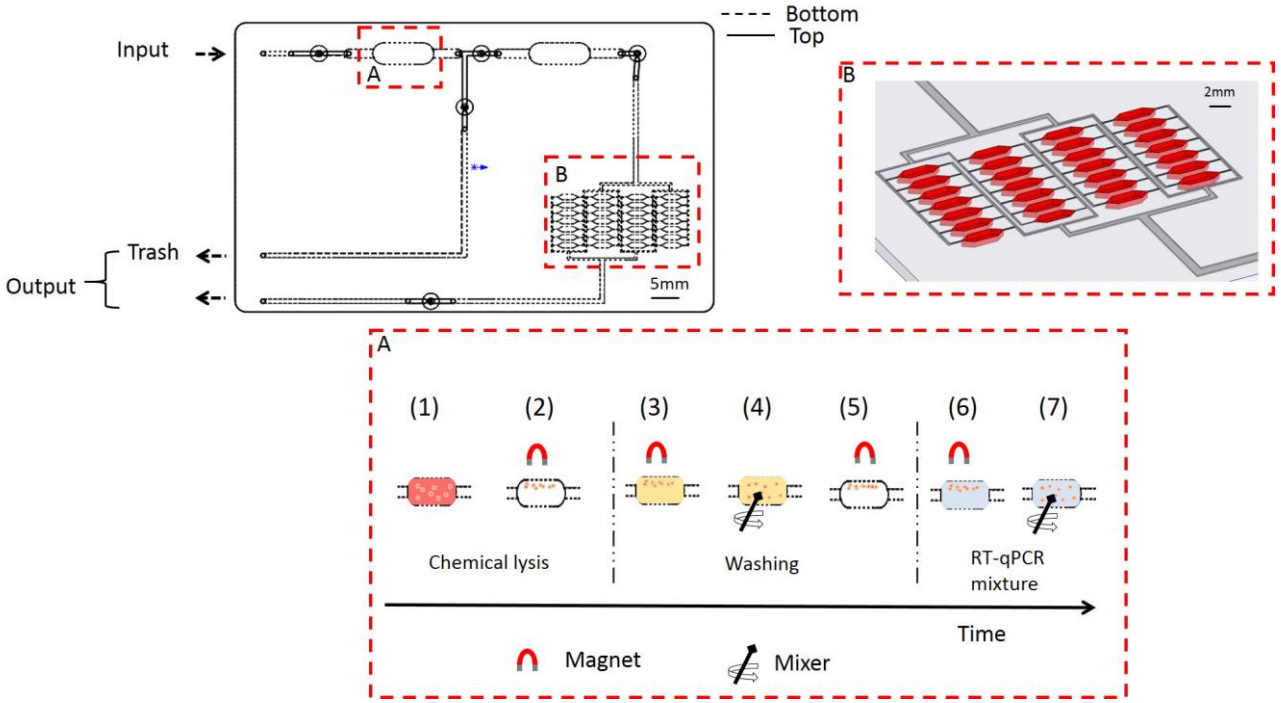

Figure2: Cartridge design and operation. The device features 3D microfluidic circuits. The top and bottom faces are connected by holes. The device consists of 1 input, 2 outputs (one for trash and the other for RT-qPCR network filling), two 80 µl chambers (one for sample preparation and an optional one for pre-filling), 28 microchambers for parallel RT-qPCR reactions, and lastly, 5 integrated valves. **A)** Schematic view of the sample preparation protocol based-on two steps: chemical lysis and washing. **Chemical lysis**: (1) Suspension consisting of a mixture of 150 µl of lysis/binding buffer, 30 µl of mouse blood from Paxgene storage (equivalent to 10 µl of whole blood), and 6 µl of Dynabeads oligo-DT are injected into chamber. (2) A magnet isolates the bead/mRNA complex in the chamber, and the chamber is flushed with air. **Washing:** (3) the washing buffer is injected into the chamber, (4) the bead/mRNA complex is mixed with the buffer and then (5) isolated with the magnet, and the chamber is flushed with air. The washing step is successively carried out two times with buffer A and once with the buffer B. (6) A suspension of RT-qPCR mix without primers/probes and sample is injected into the chamber and (7) mixed with the bead/mRNA complex. Lastly, the resulting suspension is pushed into the pre-filling chamber first, and then a pulsed-pressure is applied to simultaneously fill the network of 4X7 RT-qPCR microchambers with dried reagents for the parallel RT-qPCR reactions. A detailed description of the device operation is provided in the Supplementary information. **B)** 3D view of the RT-qPCR reaction chambers from the bottom face.

Device operation

The assembled cartridge was inserted into the developed compact instrument (see experimental set-up section in Experimental) to execute all the processes related to the diagnosis of exposure to ricin, ranging from RNA extraction from blood to tens of parallel RT-qPCR reactions. A schematic of the integrated protocol is shown in **Figure 2A**. RT was performed in one-step and directly on the bead/mRNA complex, without elution, which reduced the number of protocol steps in the cartridge. Evaporation and gas-bubble formation during PCR reactions are known limitations of performing PCR in plastic chips. These problems were counteracted by avoiding expansion of the liquid volume caused by air bubble formation, which was achieved by pressurizing the system, the tight adhesive film and the no-leakage valves.

A critical step was filling the free-valve area of the 4x7 microchamber-based RT-qPCR reactions in parallel with a single input and a single output, without trapping air and without removing the embedded primers and probes from the microchambers. We observed that air-bubbles were trapped when the flows in the branches of the network of microchambers were not synchronized. To overcome this limitation, we applied a relatively large inlet pressure (up to 1 bar) for a short time (700 milliseconds) to inject the RT-qPCR mixture with the bead/mRNA complex in the balanced network of microchambers. During the filling phase, each group of 7 microchambers was progressively filled with a reduced time delay between two adjacent microchambers. Thus, the seven different flows merge two by two at the same time and do not trap bubbles. At 1 bar

inlet pressure in our injection scheme, the flows were synchronized resulting, in complete filling of the microchambers (see **Figure S2 in the SI**; a theoretical analysis of the valve-free parallel filling of the microchambers is also provided in the SI). During injection, the high flow rate, which was estimated at 267 µl per second based on measurements from high speed camera recordings (chameleon CMLN-13S2C-CS, Edmund Optics Ltd), was fast enough to not dissolve the embedded primers and probes, but was sufficiently slow to not remove the primers and probes from the 500 µm high microchambers.

RT-qPCR microchamber-to-microchamber cross-contamination validation

Prior to validating the RT-qPCR reactions of the ricin signature in the microfluidic cartridge, we evaluated the ability of the cartridge to perform RT-qPCR reactions without microchamber-to-microchamber cross-contamination. This validation was important because the microchambers were connected by microchannels that were not isolated by valves (see **figure 2C**). With no-valves to isolate the microchambers during the RT-qPCR reactions, the elimination of microchamber-to-microchamber cross-contamination due to the reactions becomes crucial. Indeed, the exchange of minute amounts of nucleic acid between two neighboring microchambers could result in a false positive PCR outcome. The main physical phenomena that could contribute to cross-contamination are convection and diffusion. The first relies on fluid movement due to expansion of the liquid volume from air bubble formation caused by the increasing temperature during the PCR reaction. The second increases with both the nucleic acid concentration and temperature. Convection was eliminated by the no-leakage valves at the input and output of the valve-free 28 RT-qPCR reactions area. To overcome cross-contamination due to diffusion, we first optimized the design of the RT-qPCR reaction area by using high microchambers and thin microchannels. We next optimized the concentrations of the primers and probe by performing measurements of Gapdh, Stfa2 l1 and Clec4d expression using mouse total RNA. These two latter genes were randomly selected from the 27 genes of the ricin signature, and Gapdh acts as internal control. To characterize the microchamber – to – microchamber cross-contamination, various amounts of Gapdh, Stfa2 l1 and Clec4d primers/probe were embedded per cartridge according to a region of interest (ROI) boxes scheme similar to that in **Figure 3A**. The assembled cartridges were then filled with RT-qPCR suspension containing 2.5 ng/µl of mouse total RNA. Using 400 nM primers and 100 nM probe concentration, no microchamber-to-microchamber cross-contamination was observed (**Figure 3B**). The standard deviation of the threshold cycle (CT) values for each gene was less than 0.9, indicating uniform amplification across the PCR array. Finally, a comparison with similar assays performed in tubes (25µL volume) with a commercially available machine (Stratagene MX3005p, Agilent Technologies) showed similar standard deviations and sensitivity (**Figure 3C**)

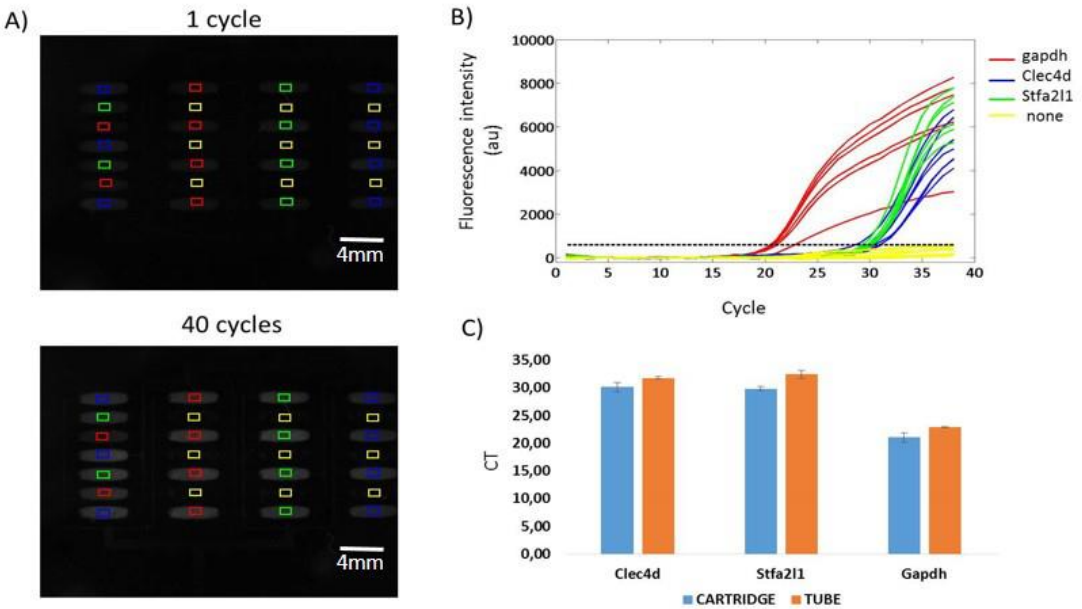

Figure3: RT-qPCR microchamber-to-microchamber cross-contamination validation. (A) Fluorescence images of the entire RT-qPCR reaction microchamber area of the microfluidic cartridge. The images were taken after 1 cycle and 40 cycles of the RT-qPCR reaction, respectively. The boxes represent the measurement window for generating the real-time RT-qPCR curves. The red, blue, and green boxes are, respectively, associated with microchambers containing embedded Gapdh, Clec4d, and Stfa2 l1 primers/probe. The yellow boxes correspond to microchambers with no primers/probe. B) Twenty eight real-time amplification curves generated by processing the entire sequence of images for the RT-qPCR microchamber-to-microchamber cross-contamination validation (from 1 cycle to 40 cycles). The threshold for determining the CT values is indicated by the dashed line. C) CT values from processing of the RT-qPCR curves in Figure 3B and similar off-chip RT-qPCR reactions. The error bars represent the standard deviation of the on-chip RT-qPCR reactions (n=6 for Gapdh, n=7 for Clec4d and n=6 for Stfa2 l1) and the off-chip RT-qPCR reactions (n=2 for Gapdh, n=2 for Clec4d, n=2 for Stfa2 l1).

Journal Name RSCPublishing

ARTICLE

Cartridge to diagnose ricin exposure

The ability of the microfluidic cartridge to diagnose ricin exposure was finally tested by performing mRNA profile measurements in blood samples collected from IOPS CD1 mice (see the blood collection section in the methods). We used IOPS CD1 mice instead of the BALBC mice previously used to establish the ricin signature to confirm the robustness and the reusability of the signature and confirm its validity, independently of the genetic background. As intranasal exposure was more toxic and is closest to the reality of a potential bioterrorist attack scenario, we chose this route of intoxication. We first performed the sample preparation off-chip, according to the scheme above for the integrated protocol in **Figure 2A**. The blood samples were collected in PAXgene tubes (BD Diagnostics, France) from six different IPOS CD1 mice (n=6) 96 hours after an intranasal exposure to ricin (n=3: 6IN, 7IN, and 8IN) and compared to a vehicle (n=3: 17IN, 18IN and 20IN). The isolated and washed bead/mRNA complex was then suspended in the RT-qPCR reaction mixture and injected into the assembled cartridge. The expression of the signature genes was considerably increased after ricin exposure (**Figure 4A**), confirming the validity of the signature. All 27 genes were upregulated in response to ricin exposure. However, three of the 27 genes were not detected in untreated mice, including the Crispld2 and Prrg2 genes in the 17IN and 18IN mice, and the Hdc gene in the 17IN mouse. The inability to detect these three genes by RT-qPCR in the cartridge was most likely due to the very low volume of the blood samples. Indeed, the signature was evaluated from only 10 µl of whole blood, limiting the quantity of mRNA available for the analysis. This quantity is also variable from one gene to the next, and from one sample to the next. Because of the lack of a comparative basis for these genes, their expression level in ricin treated mice could not be evaluated in **Figure 4A**.

We next performed the entire process of ricin exposure diagnosis in the cartridge, including RNA extraction from blood followed by 28 parallel RT-qPCR reactions. Blood samples were collected from nine different IPOS CD1 mice (n=9) in PAXgene tubes 24 hours, 48 hours and 96 hours after intranasal exposure to ricin (n=5: 3IN_24 h, 12IN_24 h, 8IN_48H, 6IN_96 h, 7IN_96 h), and compared to a vehicle (n=4:16IV_96H, 17IV_96H, 18IN_96H and 19IN_24H). All 27 genes were upregulated in response to ricin exposure. Sixteen of the 27 genes of the ricin signature were evaluated in **Figure 4B** because of the lack of a comparative basis for the other 11 genes (Oasl2, Hdc, Mmp8, Prrg2, Stfa2 l1, Anxa2, 1100001G20Rik, Clec4d, Crispld2, Ifitm2, Gp49a).

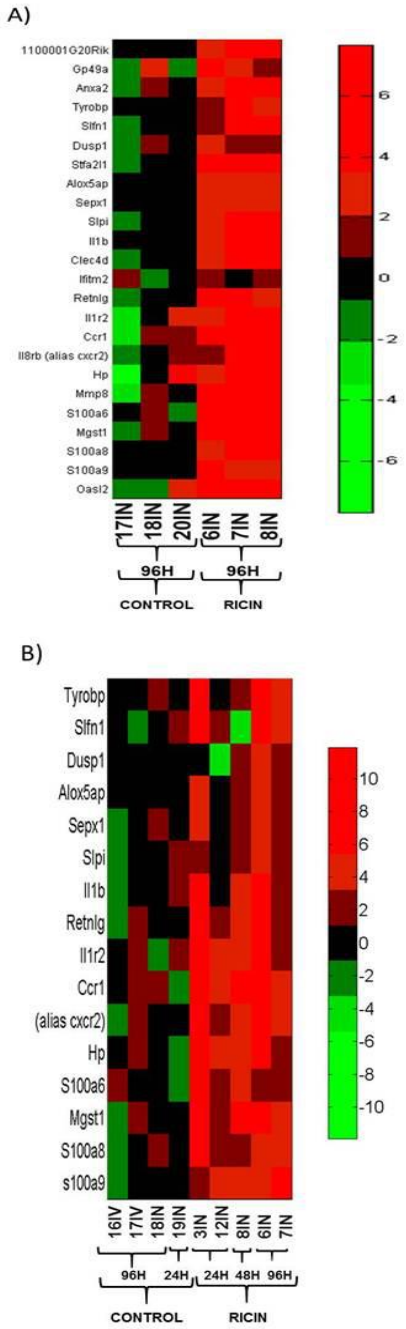

Figure 4:Real-time RT-qPCR expression profiling of ricin treated mice and untreated mice (control). A) Sample preparation off chip and RT-qPCR reaction on chip. Blood samples were collected 96 hours after exposure. B).The entire protocol steps on chip, from sample preparation to the RT-qPCR reactions. Blood samples were collected 24 hours, 48 hours and 96 hours after exposure.

These 11 genes were not detected in untreated mice, including 8 genes in 19IN_24H (Oasl2, Hdc, Mmp8, Prrg2, Stfa2 l1, Anxa2, 1100001G20Rik, Clec4d), 3 genes in 17IV_96H (Oasl2, Crispld2, Ifitm2), and 2 genes in 16IV_96H (Stfa2 l1;1100001G20Rik). Relying on the 16 detected genes, exposure to ricin was detectable within 1 h 30 min as early as 24 h after exposure (**Figure 4B**), highlighting the usefulness of this method in the early diagnosis of ricin exposure in putative victims. The intensity of upregulation for the 16 genes within the signature and the fact that we detected them as soon as 8 h (**Figure 1A**) after intranasal exposure lead us think that we could most likely detect exposure even earlier.

Conclusion

We established a new approach to diagnose exposure to ricin from a drop of blood. This approach is based on the host response to the presence of ricin in the body and has the potential to provide a comprehensive picture of the systemic response for therapeutic orientation in emergency situations. A set of 27 genes among 24109 were identified to be relevant for exposure to ricin and were validated by RT-qPCR in a microfluidic cartridge. Ricin diagnosis based on host response developed here is around 125 fold more sensitive than comparable immuno-PCR testing. However, at this stage, the signature has only been established and validated in mice, although all of the genes of the signature are also expressed in primates and human. Further developments should allow us to assess the validity of the established signature for mice in primates, or to establish a new signature in primates using the fundamental approach introduced here. Finally, it will be interesting to investigate in primates whether or not the level of gene upregulation in the signature can help clinicians to stratify patients and orient them to adequate treatment. The challenges ahead for such developments include validation studies, standardization and further development of analytical algorithms, and standardization of technical approaches for point of care testing regarding the quantity of mRNA, which can vary from one sample to the next and from one gene to the next. These variables can be critical if very low volumes of blood are used and are important in point of care applications.

The "point of care" microfluidic cartridge we proposed enables sample preparation followed by tens of parallel nucleic acid amplifications in a low-cost plastic chip. Its cost should be derisory as its fabrication is compatible with mass production by injection. The number of parallel nucleic acid amplifications in the cartridge can be considerably increased, up to several hundreds of reactions, depending on the application. The reaction volume could also be reduced to a few hundred nanoliters. The low-cost microfluidic technology developed here may find other applications in point of care diagnostics.

Acknowledgements

We are grateful for funding support from the French Alternative Energies and Atomic Energy Commission (CEA) through the Chemical, Biological, Radiological and Nuclear defense program (NRBC). We thank J-L Pesce, M. Alessio, and C. Raymond from the CEA technical support for their assistance.

Notes

[a] CEA, LETI, MINATEC Campus, 17 rue des Martyrs, F-38054 , Grenoble, Cedex 9, France.
[b] CEA, iRTSV-BGE, 17 rue des Martyrs, F-38054, F-38000 Grenoble, France.
[c] Service d'hématologie-hémostase, CHU Tours and UMR CNRS 7292, Avenue de la république 37044 Tours Cedex.
[d] Agence Nationale de sécurité de médicaments et autres produits de santé (ANSM), 635 rue de la Garenne, 34740 Vendargues.
[e] Laboratoire de Vectorologie et Thérapeutiques Anticancéreuses, Université Paris-Sud, CNRS and Gustave Roussy, UMR 8203, Villejuif, F-94805.
* Correspondence and requests should be addressed to X.G (Xavier.Gidrol@cea.fr).
†Electronic Supplementary Information (ESI) available: See DOI: 10.1039/b000000x/

References

[1] L. Montanaro, S. Sperti, A. Mattioli, G. Testonu, and F. Stirpe, "Inbibition by Ricin of Protein Synthesis in vitro," *Biochem.J*, vol. 146, no. 1975, pp. 127–131, 1975.

[2] C. L. Wilhelmsen and M. L. M. Pitt, "Lesions of Acute Inhaled Lethal Ricin Intoxication in Rhesus Monkeys," *Veterinary Pathology*, vol. 33, no. 3, pp. 296–302, May 1996.

[3] J. Men, L. Lang, C. Wang, J. Wu, Y. Zhao, P.-Y. Jia, W. Wei, and Y. Wang, "Detection of residual toxin in tissues of ricin-poisoned mice by sandwich enzyme-linked immunosorbent assay and immunoprecipitation.," *Analytical biochemistry*, vol. 401, no. 2, pp. 211–6, Jun. 2010.

[4] M. G. Poli MA, Rivera VR, Hewetson JF, "Detection of ricin by colorimetric and chemiluminescence ELISA," *Toxicon*, vol. 32, no. 11, pp. 1371–7, 1994.

[5] D. L. Brandon, "Detection of ricin contamination in ground beef by electrochemiluminescence immunosorbent assay.," *Toxins*, vol. 3, no. 4, pp. 398–408, Apr. 2011.

[6] J. S. Kim, G. P. Anderson, J. S. Erickson, J. P. Golden, M. Nasir, and F. S. Ligler, "Multiplexed Detection of Bacteria and Toxins Using a Microflow Cytometer," *Analytical chemistry*, vol. 81, no. 13, pp. 5426–5432, 2009.

[7] D. Bhatta, a a Michel, M. Marti Villalba, G. D. Emmerson, I. J. G. Sparrow, E. a Perkins, M. B. McDonnell, R. W. Ely, and G. a Cartwright, "Optical microchip array biosensor for multiplexed detection of

bio-hazardous agents.," *Biosensors & bioelectronics*, vol. 30, no. 1, pp. 78–86, Dec. 2011.

[8] B. N. Feltis, B. a Sexton, F. L. Glenn, M. J. Best, M. Wilkins, and T. J. Davis, "A hand-held surface plasmon resonance biosensor for the detection of ricin and other biological agents.," *Biosensors & bioelectronics*, vol. 23, no. 7, pp. 1131–6, Feb. 2008.

[9] W. W. Shia and R. C. Bailey, "Single domain antibodies for the detection of ricin using silicon photonic microring resonator arrays.," *Analytical chemistry*, vol. 85, no. 2, pp. 805–10, Jan. 2013.

[10] X. He, S. McMahon, T. D. Henderson, S. M. Griffey, and L. W. Cheng, "Ricin toxicokinetics and its sensitive detection in mouse sera or feces using immuno-PCR.," *PloS one*, vol. 5, no. 9, p. e12858, Jan. 2010.

[11] E. Ezan, E. Duriez, F. Fenaille, and F. Becher, *Functional Assays for Ricin Detection. In Detection of Biological Agents for the Prevention of Bioterrorism.* Springer: Netherlands, 2011, p. 131− 147.

[12] L. He, B. Deen, T. Rodda, I. Ronningen, T. Blasius, C. Haynes, F. Diez-Gonzalez, and T. P. Labuza, "Rapid Detection of Ricin in Milk Using Immunomagnetic Separation Combined with Surface-Enhanced Raman Spectroscopy," *Journal of Food Science*, vol. 76, no. 5, pp. N49–N53, 2011.

[13] S. R. Kalb and J. R. Barr, "Mass Spectrometric Detection of Ricin and its Activity in Food and Clinical Samples," *Analytical chemistry*, vol. 81, no. 6, pp. 2037–2042, 2009.

[14] S. R. Khan, A. Baghdasarian, R. P. Fahlman, K. Michail, and A. G. Siraki, "Current status and future prospects of toxicogenomics in drug discovery.," *Drug discovery today*, no. November, Nov. 2013.

[15] C. a Afshari, H. K. Hamadeh, and P. R. Bushel, "The evolution of bioinformatics in toxicology: advancing toxicogenomics.," *Toxicological sciences : an official journal of the Society of Toxicology*, vol. 120 Suppl , no. 2011, pp. S225–37, Mar. 2011.

[16] T. Veenema and J. Tõke, "Early detection and surveillance for biopreparedness and emerging infectious diseases.," *Online Journal of Issues in Nursing*, vol. 11(1):3.

[17] A. K. White, M. VanInsberghe, O. I. Petriv, M. Hamidi, D. Sikorski, M. a Marra, J. Piret, S. Aparicio, and C. L. Hansen, "High-throughput microfluidic single-cell RT-qPCR.," *Proceedings of the National Academy of Sciences of the United States of America*, vol. 108, no. 34, pp. 13999–4004, Aug. 2011.

[18] J. F. Zhong, Y. Chen, J. S. Marcus, A. Scherer, S. R. Quake, C. R. Taylor, and L. P. Weiner, "A microfluidic processor for gene expression profiling of single human embryonic stem cells.," *Lab on a chip*, vol. 8, no. 1, pp. 68–74, Jan. 2008.

[19] C. D. Chin, V. Linder, and S. K. Sia, "Commercialization of microfluidic point-of-care diagnostic devices," *Lab Chip*, vol. 12, no. 12, pp. 2118–2134, 2012.

[20] K. Ren, W. Dai, J. Zhou, J. Su, and H. Wu, "Whole-Teflon microfluidic chips.," *Proceedings of the National Academy of Sciences of the United States of America*, vol. 108, no. 20, pp. 8162–6, May 2011.

[21] E. D. Carrol, F. Salway, S. D. Pepper, E. Saunders, L. a Mankhambo, W. E. Ollier, C. A. Hart, and P. Day, "Successful downstream application of the Paxgene Blood RNA system from small blood samples in paediatric patients for quantitative PCR analysis.," *BMC immunology*, vol. 8, p. 20, Jan. 2007.

[22] K. Le Brigand, R. Russell, C. Moreilhon, J.-M. Rouillard, B. Jost, F. Amiot, V. Magnone, C. Bole-Feysot, P. Rostagno, V. Virolle, V. Defamie, P. Dessen, G. Williams, P. Lyons, G. Rios, B. Mari, E. Gulari, P. Kastner, X. Gidrol, T. C. Freeman, and P. Barbry, "An open-access long oligonucleotide microarray resource for analysis of the human and mouse transcriptomes.," *Nucleic acids research*, vol. 34, no. 12, p. e87, Jan. 2006.

[23] Y. Benjamini and Y. Hochberg, "Controlling the false discovery rate: a practical and powerful approach to multiple testing," *Journal of the Royal Statistical Society, Series B*, vol. 57 (1), pp. 289–300, 1995.

[24] T. D. Schmittgen and K. J. Livak, "Analyzing real-time PCR data by the comparative CT method," *Nature Protocols*, vol. 3, no. 6, pp. 1101–1108, Jun. 2008.

